THE FASEB JOURNAL • RESEARCH • www.fasebj.org

# Structure of YidC from *Thermotoga maritima* and its implications for YidC-mediated membrane protein insertion

**Yanlong Xin,[*,†] Yan Zhao,[†] Jiangge Zheng,[†] Haizhen Zhou,[†] Xuejun Cai Zhang,[†,‡] Changlin Tian,[*,§,1] and Yihua Huang[†,‡,2]**

[*]National Laboratory for Physical Science at Microscale, School of Life Science, University of Science and Technology of China, Hefei, China; [†]National Laboratory of Biomacromolecules, Chinese Academy of Sciences Center for Excellence in Biomacromolecules, Institute of Biophysics, Chinese Academy of Sciences, Beijing, China; [‡]University of Chinese Academy of Sciences, Beijing, China; and [§]High Magnetic Field Laboratory, Chinese Academy of Sciences, Hefei, China

**ABSTRACT: The evolutionarily conserved YidC/Oxa1/Alb3 family of proteins represents a unique membrane protein family that facilitates the insertion, folding, and assembly of a cohort of α-helical membrane proteins in all kingdoms of life, yet its underlying mechanisms remain elusive. We report the crystal structures of the full-length *Thermotoga maritima* YidC (TmYidC) and the TmYidC periplasmic domain (TmPD) at a resolution of 3.8 and 2.5 Å, respectively. The crystal structure of TmPD reveals a β-supersandwich fold but with apparently shortened β strands and different connectivity, as compared to the *Escherichia coli* YidC (EcYidC) periplasmic domain (EcPD). TmYidC in a detergent-solubilized state also adopts a monomeric form and its conserved core domain, which consists of 2 loosely associated α-helical bundles, assemble a fold similar to that of the other YidC homologues, yet distinct from that of the archaeal YidC-like DUF106 protein. Functional analysis using *in vivo* photo-crosslinking experiments demonstrates that Pf3 coat protein, a Sec-independent YidC substrate, exits to the lipid bilayer laterally *via* one of the 2 α-helical bundle interfaces: TM3–TM5. Engineered intramolecular disulfide bonds in TmYidC, in combination with complementation assays, suggest that significant rearrangement of the 2 α-helical bundles at the top of the hydrophilic groove is critical for TmYidC function. These experiments provide a more detailed mechanical insight into YidC-mediated membrane protein biogenesis.—Xin, Y., Zhao, Y., Zheng, J., Zhou, H., Zhang, X. C., Tian, C., Huang, Y. Structure of YidC from *Thermotoga maritima* and its implications for YidC-mediated membrane protein insertion. FASEB J. 32, 2411–2421 (2018). www.fasebj.org**

**KEY WORDS: X-ray crystallography · YidC/Oxa1/Alb3 · membrane protein insertase · membrane protein biogenesis**

In eubacteria, membrane proteins account for ~30% of the total proteins synthesized in the cell. The YidC/Oxa1/Alb3 family of proteins, which shares no sequence identity and has substrates distinct from those of other membrane protein insertion mechanisms, such as the Sec61/SecYEG translocon (1) and the Get1/2 complex (2), represents a unique membrane protein family that facilitates the insertion, folding, and assembly of a cohort of α-helical membrane proteins (3–5). In prokaryotes, the YidC proteins promote the insertion of proteins into the bacterial cytoplasmic membrane, either independently (6) or cooperatively, with the SecYEG translocon (7), whereas, in eukaryotes, the mitochondrial Oxa1 and chloroplast Alb3 homologues catalyze the insertion of proteins into the inner membrane of mitochondria and the thylakoid membrane of chloroplast, respectively (3, 5). Despite the presence of an extra transmembrane (TM) helix and a large periplasmic domain (PD) at the N terminus in Gram-negative bacterial YidC homologues (8), a signature of the YidC/Oxa1/Alb3 family proteins is the presence of a conserved C-terminal core domain that consists of 5 TM segments, an essential domain for its membrane insertase activity.

**ABBREVIATIONS:** BhYidC, *Bacillus halodurans* YidC; BPA, benzoyl-L-phenylalanine; DM, *n*-decyl-β-D-maltopyranoside; EcPD, *Escherichia coli* YidC periplasmic domain; EcYidC, *Escherichia coli* YidC; IPTG, isopropyl β-D-thiogalactoside; LB, Luria Bertani; LDAO, lauryldimethylamine-*N*-oxide; pBPA, *p*-benzoyl-L-phenylalanine; PD, periplasmic domain; TM, transmembrane; TmPD, *Thermotoga maritima* YidC periplasmic domain; TmYidC, *Thermotoga maritima* YidC

[1] Correspondence: Hefei National Laboratory for Physical Sciences at Microscale, School of Life Sciences, University of Science and Technology of China, Hefei, 230026, China. E-mail: cltian@ustc.edu.cn

[2] Correspondence: National Laboratory of Biomacromolecules, CAS Center for Excellence in Biomacromolecules, Institute of Biophysics, Chinese Academy of Sciences, No. 15 Datun Rd., Chaoyang District, Beijing 100101, China. E-mail: yihuahuang@sun5.ibp.ac.cn

doi: 10.1096/fj.201700893RR

This article includes supplemental data. Please visit *http://www.fasebj.org* to obtain this information.

Recent structural and functional studies have greatly advanced our understanding of the molecular mechanisms underlying the YidC/Oxa1/Alb3–mediated membrane protein biogenesis. Ravaud *et al*. (9) and Oliver *et al*. (10) independently determined the crystal structures of the isolated large *Escherichia coli* YidC (EcYidC) PD (EcPD), revealing a β-supersandwich fold commonly seen in sugar-binding proteins, yet its exact function remains elusive. Using cryo electron microscopy methods, several groups reported the structure of ribosome nascent chain-bound YidC, but the oligomerization state of YidC in the cotranslational translocon remains controversial (11–14). Breakthroughs have been made recently by Kumazaki *et al*. (15, 16), who determined the high-resolution crystal structures of the Gram-positive bacteria *Bacillus halodurans* YidC2 (BhYidC) and the Gram-negative bacteria EcYidC, both crystallized as monomers by the lipidic cubic phase method, revealing that both BhYidC and EcYidC contain 5 conserved TM helices that assemble to form a substrate-loading hydrophilic groove in the inner leaflet of the bilayer, open to both the cytoplasm and the lipid bilayer. Combined with functional analysis, they further demonstrated that a conserved positively charged residue in the hydrophilic groove plays a critical role in attracting substrates. More recently, Borowska *et al*. (17) determined the crystal structure of the archaeal DUF106 protein, a YidC-like membrane protein, from *Methanocaldococcus jannaschii* (Mj0480) in a detergent-solubilized state. Intriguingly, distinct from BhYidC and EcYidC, the DUF106 protein oligomerizes to form a tetramer in the crystal structure and possesses only 3 TM segments that correspond to the location of TM2, -3, and -6 of the EcYidC, but exhibiting a certain degree of structural similarities to the core region of EcYidC and BhYidC (18).

Despite this significant progress, some important questions on how the YidC/Oxa1/Alb3 proteins facilitate membrane protein substrate insertion in the membrane remain open. First, the substrate-loading hydrophilic groove assembled by the 5 conserved TM segments in all the reported YidC homologue structures remains closed to the periplasmic space, and it is unclear whether conformational changes are necessary to promote substrate entry into the groove and release into the membrane. Second, both BhYidC and EcYidC structures illustrate that the architecture of the core domain consists of 2 α-helical bundles that are loosely associated *via* the TM3–TM5 interface and the opposite TM2–TM6 interface in EcYidC (or the TM2–TM4 interface and the TM1–TM5 interface in BhYidC). Which interface serves as the substrate exit gate remains to be resolved. In addition, YidC proteins appear to adopt different conformations and oligomerization states in the detergent-solubilized state and in a lipidic environment (12–16, 19). It is unclear whether detergents and lipids have different effects on the oligomerization states and conformational states of YidC proteins. To clarify these questions, we determined the crystal structures of the full-length *Thermotoga maritima* YidC (TmYidC) and the TmYidC PD (TmPD) at a resolution of 3.8 and 2.5 Å, respectively. Intriguingly, despite no amino acid sequence identity between EcPD and TmPD, crystal structure reveals that TmPD also forms a β-supersandwich fold but with apparently shortened β strands; TmYidC in a detergent-solubilized state adopts a monomeric form, and its conserved core domain arranges to form a fold similar to that of the other YidC homologues, yet distinct from that of the archaeal YidC-like DUF106 protein. Functional analysis using *in vivo* photo-crosslinking experiments demonstrates that the Pf3 coat protein, a Sec-independent YidC substrate, exits to the lipid bilayer laterally at the TM3–TM5 interface, but not at the TM2–TM6 interface, of TmYidC. Engineered intramolecular disulfide bonds in TmYidC, in combination with complementation assays, suggest that significant rearrangement of the 2 α-helical bundles at the top of the hydrophilic groove is critical for TmYidC function.

## MATERIALS AND METHODS

### Protein expression, purification, and structure determination of TmPD and TmYidC

The full-length *yidC* gene was amplified by the standard PCR method from the genomic DNA of *T. maritima* (American Type Culture Collection, Manassas, VA, USA). The amplified fragment was subcloned into the pET-20b vector (Novagen, Darmstadt, Germany) *via* restriction enzymes *Nde*I and *Xho*I. The generated plasmid pET20b-TmYidC contains a $His_6$ tag at the C terminus of TmYidC to facilitate protein affinity purification. The sequence of *yidC* from *T. maritima* was then verified by DNA sequencing. The pET20b-TmYidC plasmid was transformed into BL21 (DE3) for protein expression. Cells were grown in Luria Bertani (LB) medium supplemented with ampicillin (50 mg/ml) at 37°C to an absorbance at an optical density at 600 nm ($OD_{600}$) of 1.0, induced with 0.3 mM IPTG for 6 h at 30°C, and harvested by centrifugation at 4500 *g* for 30 min at 4°C. Cell pellets were resuspended in PBS (pH 7.5), lysed by sonication (Misonix SonicatorS-4000; Cole Parmer, Vernon Hills, IL, USA), and centrifuged at 39,000 *g* for 1 h at 4°C, to collect the total cell membranes. The membrane fraction was subsequently resuspended in PBS (pH 7.5) supplemented with 1% (w/v) lauryldimethylamine-*N*-oxide (Anatrace, Maumee, OH, USA) and 50 mM imidazole and was solubilized for 2 h at 4°C. The supernatant was collected after another centrifugation at 39,000 *g* for 1 h, and affinity purified on a HiTrap nickel column (GE Healthcare, Waukesha, WI, USA). TmYidC protein bound on the nickel column was washed with 3 column volumes of washing buffer that contains PBS (pH 7.5) and 0.5% (w/v) *n*-decyl-β-D-maltopyranoside (DM; Anatrace), to change the detergent, and was subsequently eluted off the column with buffer containing PBS (pH 7.5), 300 mM imidazole, and 0.25% (w/v) DM. The eluted protein was concentrated in a 50 kDa cutoff concentrator (Thermo Fisher Scientific, Waltham, MA, USA) and loaded onto a Superdex-200 size-exclusion column (GE Healthcare) that was pre-equilibrated with a buffer containing 20 mM Tris-HCl (pH 8.0), 150 mM NaCl, 0.2% (w/v) DM. The peak fractions were collected and concentrated to ~10 mg/ml for crystallization.

For constructing plasmid pET20b-TmPD that expresses the PD of TmYidC, the DNA sequence encoding residues 24–222 of TmYidC was amplified from the full-length *yidC* and subsequently subcloned into a pET20b vector *via* restriction enzyme sites *Nde*I and *Xho*I, with a C-terminal $His_6$ tag to facilitate affinity purification. The constructed plasmid pET20b-TmPD was transformed into BL21 (DE3) for protein expression. Cells were grown in LB supplemented at 37°C to an absorbance at $OD_{600}$ of 1.5, induced with 0.3 mM IPTG overnight at 30°C, and harvested by centrifugation at 4500 *g* for 30 min at 4°C. Cell pellets were resuspended in PBS (pH 7.5), lysed by sonication, and then

centrifuged at 39,000 *g* for 1 h at 4°C to collect the supernatant. After incubation with Nickel NTA agarose beads (Gold Biotechnology, Olivette, MO, USA) for 1 h at 4°C, the TmPD-bound beads were washed with 3 column volumes of washing buffer that contained PBS (pH 7.5) and 10 mM imidazole. After 2 washes, TmPD protein was eluted off the beads with a buffer containing PBS (pH 7.5) and 300 mM imidazole. The eluted protein was concentrated in a 30 kDa cutoff concentrator and loaded onto a Superdex-200 size-exclusion column that was pre-equilibrated with a buffer containing 20 mM Tris-HCl (pH 8.0), and 150 mM NaCl. The peak fractions were collected and concentrated to ~20 mg/ml for crystallization.

Se-Met substituted TmYidC and TmPD protein were prepared by using the same procedures as described above for the native TmYidC and TmPD protein, respectively. To obtain phases for structure determination of TmPD, 3 Met mutations (L57M, I105M, and L153M) were introduced into the native sequence by standard PCR protocol, because TmPD contains only 1 Met residue (M194) in its native sequence.

Crystallization was conducted at 16°C using the hanging drop vapor diffusion method by mixing the protein and precipitants at a ratio of 1:1. Both native TmPD crystals and Se-Met substituted TmPD crystals were obtained in a crystallization condition containing 0.05 M glycine (pH 9.0) and 55% PEG400 (w/v); The best TmYidC crystals were obtained in a solution containing 0.1 M HEPES (pH 7.5) and 20% PEG1500 (w/v) within 2 wk. Selenomethionyl TmYidC crystals were obtained in a similar condition. The selenomethionyl data of TmPD and TmYidC were collected at a wavelength of 0.9792 Å, which corresponded to their anomalous dispersion peak wavelength. The diffraction resolutions of the selenomethionine derivative TmPD and TmYidC crystals were up to 2.5 and 3.8 Å, respectively. All the datasets were collected at the beamline BL-17U (Synchrondron Radiation Facility; Shanghai, China), and processed using HKL2000 (20). The TmPD and TmYidC crystals belonged to space groups $P4_1$ and $P2_12_12_1$, respectively.

Experimental phases of TmPD structure were obtained using the single-wavelength anomalous dispersion method. Four Se-Met sites for each of the TmPD monomer were quickly located by using Shelx-D in the Phenix package (21). Phenix was used to refine the sites and calculate phases (22). The initial model was built using the program Phenix.autobuild, and the model was improved by iterative cycles of manual fitting with COOT (23). Model validation was performed using the Molprobity server. The final model had $R_{work}$ and $R_{free}$ of 0.22 and 0.26, respectively. The TmYidC structure was determined with molecular replacement (MR) using the isolated TmPD and BhYidC (PDB ID: 3WO6) structures as search models. The final model was refined to 3.8 Å resolution with $R_{work} = 0.27$ and $R_{free} = 0.31$. The registry in the core domain of the TmYidC was further validated using the 4 peaks in the Se Fourier maps at a contour level of 3.0 σ. All structural figures were prepared with PyMol (24). X-ray data and refinement statistics are given in **Table 1**.

## Construction of the *yidC*-depleted *E. coli* strain

The chromosomal *yidC* gene of *E. coli* strain BW25113 was deleted by the Datsenko-Wanner knockout system (25). In brief, the chloramphenicol resistance gene was amplified from the pKD3 plasmid by PCR, using the primers that include 20 nt of priming sites of chloramphenicol resistance gene and 60 nt from each side of the *yidC* gene. The PCR products were subsequently transformed into *E. coli* BW25113 cells that carried both the pBAD-*yidC* plasmid ($Kan^+$) and the pKD46 plasmid ($Amp^+$). The resulting recombinants, in which the chromosomal *yidC* gene was replaced with chloramphenicol resistance gene by homologous recombination, were isolated by plating on LB agar at 37°C in the presence of L-arabinose (0.2%, v/w),

TABLE 1. *Data collection and refinement statistics*

| Parameter | SeMet-TmYidC | TmYidC | SeMet-TmPD |
|---|---|---|---|
| Data collection | | | |
| Space group | $P2_12_12_1$ | $P2_12_12_1$ | $P4_1$ |
| Cell dimensions | | | |
| *a*, *b*, *c* (Å) | 75.7, 103.6, 129.7 | 75.5, 102.9, 130.1 | 79.9, 79.9, 135.8 |
| α, β, γ (deg) | 90.0, 90.0, 90.0 | 90.0, 90.0, 90.0 | 90.0, 90.0, 90.0 |
| Wavelength (Å) | 0.97920 | 0.81523 | 0.97915 |
| Resolution (Å) | 50–3.80 (3.94–3.80) | 50–4.00 (4.14–4.00) | 29.11–2.50 (2.54–2.50) |
| $R_{sym}$ | 0.120 (1.0) | 0.098 (0.9) | 0.129 (1.0) |
| $I/\sigma$ | 14.5 (1.0) | 21.8 (2.7) | 16.6 (2.1) |
| $CC_{1/2}$ (%) | 100 (53) | 100 (88) | 100 (71) |
| Redundancy | 8.2 (8.3) | 7.0 (7.1) | 10.2 (9.6) |
| Completeness (%) | 99.7 (100) | 99.6 (100) | 99.9 (99.9) |
| Sites (*n*) | 5 | | 4 |
| Refinement | | | |
| Resolution (Å) | 3.80 | | 2.50 |
| Reflections (*n*) | 14,133 | | 25,450 |
| $R_{work}/R_{free}$ | 26.9/31.3 | | 22.1/26.1 |
| Atoms (*n*) | 2680 | | 6555 |
| B-factors | 69.7 | | 34.5 |
| RMS deviations | | | |
| Bond lengths (Å) | 0.01 | | 0.01 |
| Bond angle (deg) | 1.37 | | 0.86 |
| Ramachandran plot | | | |
| Favored (%) | 90.8 | | 91.2 |
| Allowed (%) | 7.4 | | 8.2 |
| Outliers (%) | 1.8 | | 0.6 |

The numbers in parentheses denote the highest resolution shell.

chloramphenicol (24 μg/ml), and kanamycin (25 μg/ml). Followed by growing on LB agar at 42°C to eliminate the pKD46 plasmid, the resulting clones were transformed with pCP20 plasmid to remove the chloramphenicol resistance gene. pCP20 plasmids in the recombinants were further eliminated by growing on LB agar plate at 42°C overnight. The constructed *yidC*-depleted *E. coli* BW25113 strain was confirmed by PCR.

### *In vivo* photo-crosslinking of Ec-Tm YidC fusion protein and its substrate Pf3 coat protein

The coding sequence of Pf3 coat protein with a C-terminal Flag tag and a preceding *Taq* promoter and the Ec-Tm *yidC* fusion gene plus its endogenous promoter were subcloned into pCDFDuet vector (Novagen) using restriction enzymes *Nde*I/*Xho*I and *Eco*RI/*Not*I, respectively. The generated pCDFDuet-Pf3-YidC plasmid contained a Flag tag at the C terminus of Pf3 for immunoblot detection. The amber TAG codon was introduced into the indicated position in pCDFDuet-Pf3-YidC plasmid by site-directed mutation mutagenesis. All of the mutations were confirmed by DNA sequencing. Two plasmids pCDFDuet-Pf3-YidC and pSup-BpaRS-6TRN were cotransformed into the *yidC*-depleted *E. coli* strain for *in vivo* photo-crosslinking experiments.

The *yidC*-depleted *E. coli* that carries 2 plasmids, pSup-BpaRS-6TRN and pCDFDuet-Pf3-YidC, was grown in LB medium in the presence of chloramphenicol (25 μg/ml), streptomycin (100 μg/ml), and benzoyl-L-phenylalanine (BPA; 1 mM; Bachem, Bubendorf, Switzerland), at 37°C in the dark. Pf3 expression was induced by addition of 1 mM IPTG at cell density of 0.4 ($OD_{600}$) for 10 min. Subsequently, cells were transferred to a 6-well microtiter plate and exposed to a UV lamp (365 nm, 100 W; Thermo Fisher Scientific) for 20 min. Nonradiated samples were taken as a control. Followed by membrane solubilization with 1% lauryldimethylamine-*N*-oxide (w/v), sample supernatants were subject to SDS-PAGE analysis and immunoblot analysis with anti-Flag tag mAb (AP1013a; Abgent, San Diego, CA, USA) for detection.

### Complementation assay

The rescue plasmid was constructed by inserting the full-length *E. coli yidC* gene, *T. maritima yidC* gene, or Ec-Tm *yidC* fusion gene with a C-terminal $His_6$ tag coding sequence and its endogenous promoter as well as a ribosome-binding site into the pACYC184 vector (New England Biolabs, Ipswich, MA, USA), which is a low-copy-number plasmid. The pACYC184-Ec-Tm YidC plasmid was then used as a template to make all the mutants. All of the mutations were confirmed by sequencing.

To perform a complementation assay, the *yidC*-depleted *E. coli* strain was transformed with plasmids expressing either the wild-type Ec-Tm YidC or various Ec-Tm YidC mutants and plated on LB agar that was supplemented with L-arabinose (0.2%, w/v), chloramphenicol (24 μg/ml), and kanamycin (25 μg/ml) at 37°C overnight. A single colony was picked from the plate and inoculated in 5 ml LB medium supplemented with chloramphenicol (24 μg/ml), kanamycin (25 μg/ml), and L-arabinose (0.2%, w/v) at 37°C for about 6 h. When cell density reached an $OD_{600}$ of 1.0, the cells were spun down to remove the growth medium, followed by washing twice with fresh LB that did not contain any antibiotics and L-arabinose, and cell density was adjusted to 0.5 ($OD_{600}$). For each sample, a serial dilution (1:10, 1:100, 1:1000, 1:10000, and 1:100000) was made, and 1 μl of each diluted sample was spotted onto LB plates containing antibiotics (25 μg/ml kanamycin and 24 μg/ml chloramphenicol), with or without L-arabinose (0.2%, v/w). Lack of L-arabinose in the LB medium strictly inhibited the expression of EcYidC from the pBAD-EcYidC plasmid. The plates were incubated overnight at 37°C. The complementation assays were repeated at least 3 times. Membrane fractions of cell lysates were collected and subjected to SDS-PAGE and anti-His immunoblot analysis. Expression levels of selected inactive mutations were verified with immunoblot analysis.

### Western blot analysis

Western blot analyses were performed to compare protein expression levels of the wild-type Ec-Tm *yidC* fusion and its various mutants. To compare protein expression levels, plasmids expressing the wild-type or various mutants were transformed into the *yidC*-depleted *E. coli* strain and spread on LB agar plates that contained chloramphenicol (24 μg/ml) and kanamycin (25 μg/ml). After incubation at 37°C for 12 h, colonies were scraped off the plates and transferred to Eppendorf tubes (Millipore-Sigma, Billerica, MA, USA), and the cell density was adjusted to $OD_{600}$ of 1.0 by addition of 1× PBS buffer. Cells (10 μl) from each sample were allocated into Eppendorf tubes and heated at 100°C for 5 min before SDS-PAGE analysis. After electrophoresis, the proteins were transferred to a PVDF membrane and blocked with TBST buffer [20 mM Tris-HCl (pH 8.0), 150 mM NaCl, 0.05% Tween-20] that contained 5% skim milk for 1 h. The PVDF membrane containing YidC proteins was then incubated with anti-His mouse mAb (1:3000; Tiangen, Sichuan, China) at room temperature for 1 h and subsequently washed with TBST buffer twice and further incubated with horseradish-peroxidase–conjugated secondary antibody (1:3000; HS201; TransGen Biotech, Beijing, China) at room temperature for 1 h. For the PVDF membrane containing Pf3 proteins, FLAG tag antibody (AP1013a; Abgent) was used as the primary antibody and horseradish peroxidase–conjugated antibody (1:3000; HS101; Trans) as the secondary antibody. PVDF membranes were exposed by using ECL reagents (EasySee Western Blot Kit, TransGen Biotech). For those mutants that are unable to rescue the growth of the *yidC*-depleted *E. coli* strain on LB agar plates without addition of L-arabinose, cells were withdrawn from their corresponding LB agar plates that contained 0.2% L-arabinose, chloramphenicol (24 μg/ml), and kanamycin (50 μg/ml).

## RESULTS

### Crystal structures of the PD and the full-length YidC from *T. maritima*

The cloning, overexpression, purification, and crystallization of TmPD, including residues 24–222, and the full-length YidC from *T. maritima* were performed as described in the Materials and Methods section. Similar to EcYidC, TmYidC has a molecular mass of 51.2 kDa and consists of 6 TMs and a large PD that is inserted between TM1 and -2 of TmYidC (**Fig. 1*A***). Sequence alignment indicates that the conserved C-terminal core domain of TmYidC shares 32% amino acid sequence identity to that of EcYidC, but the TmPD domain exhibits no sequence similarity to EcPD.

To facilitate the determination of the structure of full-length TmYidC, we first identified the crystal structure of the isolated TmPD domain that covers residues 24–222. TmPD was crystallized in a space group $P4_1$ with 4 molecules in 1 asymmetric unit. The structure was determined with the selenomethionine-based, single wavelength anomalous dispersion method by introducing 3 extra Met mutations (L57M, I105M, and L153M) in the wild-type

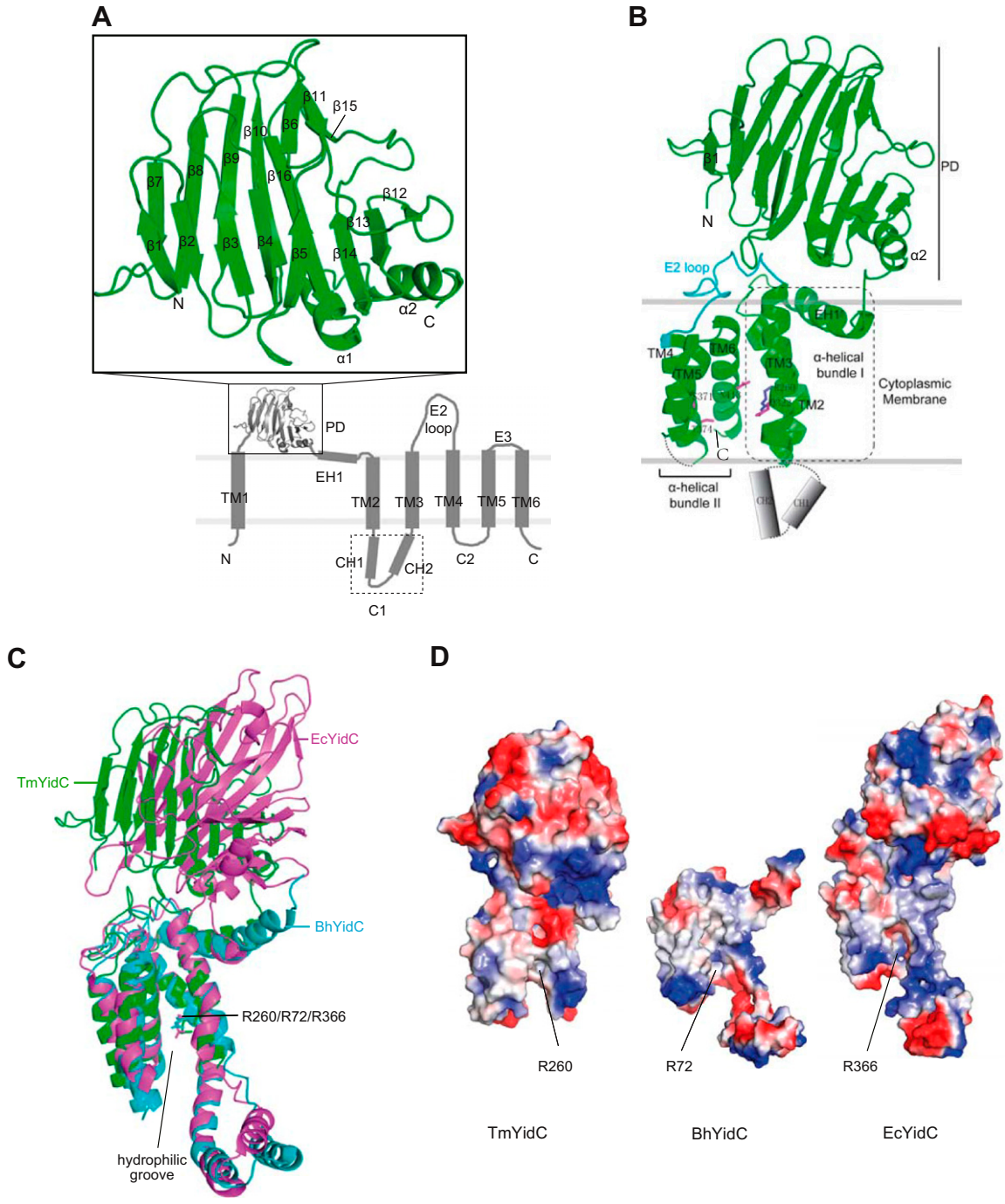


**Figure 1.** Crystal structures of TmPD and TmYidC. *A*) A topology diagram of the full-length TmYidC based on prediction. Helices are indicated by cylinders. TmYidC contains 6 TM segments (TM1–6), an amphipathic EH1 helix and a PD that inserts between TM1 and -2. The CH1 and -2 helices in the cytosolic loop C1 fold into a hairpin-like structure. The inset shows the crystal structure of TmPD (residues 24–222). *B*) Overall structure of TmYidC in cartoon representation. The core domain of TmYidC consists of 2 α-helical bundles (α-helical bundle I: EH1, TM2, and TM3; α-helical bundle II: TM4, -5, and -6). The 2 α-helical bundles are connected by the E2 loop (in cyan). The TM1 (residues 1–23), C1 region (residues 271–315), C2 loop (residues 378–388), and C terminus (residues 423–445) of TmYidC are disordered in structure. Hydrophilic residues (S371, T374, N413, R260, and Q322) in the hydrophilic groove are labeled. The 2 interfaces of the 2 α-helical bundles are the TM3–TM5 interface and the TM2–TM6 interface. *C*) Overlay of BhYidC (cyan), EcYidC (magenta), and TmYidC (green): the conserved core domain of the 3 YidC proteins resembles one another; the conserved positively charged residues in 3 proteins are located in a similar position in the hydrophilic groove. *D*) Electrostatic representation showing the interior surface features of the hydrophilic groove in 3 YidC proteins.

sequence for phasing, as there is only 1 Met residue (M194) in the TmPD native sequence. The final model was refined to 2.5 Å resolution with a seleno-derived dataset, to $R_{work}$ = 22.1% and $R_{free}$ = 26.1% (Table 1). In the crystal, the 4 molecules, related by a 4-fold non-crystallographic symmetry axis, are almost identical to each other with a root mean square deviation (rmsd) of ~0.6 Å for all 199 aligned Cα atoms.

Overall, TmPD consists of 2 twisted antiparallel β-sheets (S1 and S2) and 2 C-terminal short α helices (α1 and α2) (Fig. 1*A* and Supplemental Fig. S1*A*). S1 (8-stranded β-sheet: β1–6, -11 and -15) and S2 (8-stranded β-sheet: β7–10, -12–14, and -16) pack against each other and form a β-supersandwich fold (Fig. 1*A*). The C terminus of the TmPD structure (residues 198–222) consists of the helices α1 and α2, which are packed against the S2 layer of the β-supersandwich (Fig. 1*A*). Although TmPD shares no sequence identity with EcPD, it folds as a β-supersandwich but with shorter lengths of the β-strands and different connectivities. These remarkable differences resulted in failure to solving the TmPD structure by molecular replacement using the EcPD structure (PDB IDs: 3BS6 or 3BLC) as a search model. Unlike EcPD structure, TmPD lacks the characteristic concave surface, a large cleft that potentially serves as a sugar-binding pocket in galactose mutarotase (9, 10) (Supplemental Fig. S1*B*). In addition, SecYEG and SecDFYajC, components of the holotranslocon that consists of single copies of YidC, SecYEG, and SecDFYajC, were reported to interact with part of the PD domain (residues 215–265) of EcYidC (Supplemental Fig. S1*B*), yet this interacting region is also not conserved in the TmPD structure, suggesting that the PD domains of YidC proteins bind SecYEG and SecDFYajC components *via* nonconserved, interacting surfaces (7, 26, 27).

The full-length TmYidC was crystallized in an *n*-decyl-β-D-maltopyranoside (DM)–containing solution, and its structure was determined by molecular replacement, using the isolated TmPD and BhYidC (PDB ID: 3WO6) structures as search models. The final model was refined to 3.8 Å resolution with $R_{work}$ = 26.9% and $R_{free}$ = 31.3% (Table 1). The register of the resulting model was further confirmed by the 5 selenomethionine positions located from a selenomethionyl crystal (Supplemental Fig. S2*A*).

In the crystal lattice, the TmYidC molecules appeared to exist as monomers, in agreement with the observations in the crystal structures of BhYidC and EcYidC that were crystallized in a lipidic environment (15, 16). This observation further supports that YidC may function as monomers, in line with the recent findings that monomeric EcYidC binds to translating ribosomes in a detergent-solubilized state (11, 14).

Intriguingly, the TM1 helix and the following N-terminal region of the PD domain (residues 1–21) were disordered in the TmYidC structure (Fig. 1*B*). N-terminal sequencing confirmed that these TM1 residues were intact in the crystallized TmYidC protein, a scenario that was also observed in EcYidC structure (16). Intriguingly, apart from the N terminus of TmYidC (residues 1–21), the cytoplasmic regions of TmYidC, which include the C1 region (residues 271–315); C2 loop (residues 378–388), which connects TM4 and -5; and the C-terminal loop (residues 423–445) are all invisible in the structure, suggesting that these cytoplasmic regions are highly dynamic, in accordance with previous structural analyses of EcYidC and BhYidC (15, 16).

Overall, similar to EcYidC structure, TmYidC comprises an N-terminal protruding PD domain in the periplasm and C-terminal 5 TM segments (TM2–6), connected by the amphipathic EH1 helix, lying parallel to the plane of the membrane (Fig. 1*B*). The 5 TM segments are tightly packed together on the periplasmic side, but loosely interact with each other on the cytoplasmic side, creating a groove that is open to cytoplasm and inner leaflet of the cytoplasmic membrane (Fig. 1*B*). The architecture of the core domain of TmYidC has a topology similar to that of BhYidC and EcYidC, consisting of 2 loosely associated α-helical bundles—α-helical bundle I (EH1, TM2, and TM3) and α-helical bundle II (TM4, -5, and -6)—connected by a long periplasmic loop E2 (Fig. 1*B*). Examination of the interfaces between the 2 α-helical bundles indicates that only 3 pairs of residues are in Van der Waals contact between TM2 and -6, and no contacts are found between TM3 and -5, suggesting that both the TM2–TM6 and TM3–TM5 interfaces could serve as substrate exit gates. The hydrophilic groove of TmYidC contains several hydrophilic residues, including S371, T374, N413, R260, and Q322 (15, 16, 28) (Fig. 1*B*). In particular, the highly conserved positively charged residue R260 that sits on the TM2 is located at the heart of the hydrophilic groove.

Structural comparisons indicate that the PD domain in the TmYidC structure is essentially identical to the isolated TmPD structure with an rmsd of 0.46 Å over the 199 aligned Cα atoms. By contrast, the TmPD domain is not superimposable on the EcPD structure. Overlay of the conserved core domain structure of TmYidC with that of EcYidC and BhYidC reveals that the EH1 helix and 5 TM segments adopt a quite similar conformation, with rmsd of 1.2 and 1.1 Å, respectively, over the 100 aligned Cα atoms (Fig. 1*C*). Electrostatic representation of TmYidC, BhYidC, and EcYidC indicates that the hydrophilic substrate-loading groove has similar interior surface properties and opens to both cytoplasm and the lipid bilayer (Fig. 1*D*). These features suggest that this functionally important core domain of YidC proteins is conserved, both structurally and in primary sequence.

## The substrate exit gate is located at the TM3–TM5 interface in the C-terminal core domain of TmYidC

Similar to the BhYidC and EcYidC structures, the conserved core domain of TmYidC consists of 2 helical bundles, each containing 3 α helices (α-helical bundle I: EH1, TM2, and -3; α-helical bundle II: TM4, -5, and 6; Fig. 1*B, C*). The 2 α-helical bundles are connected by a long periplasmid loop E2 at the top of the hydrophilic groove on the periplasmic side. Packing of the 2 helical bundles generates 2 potential substrate exit gates: the TM3–TM5 interface and the TM2–TM6 interface, raising the question of which interface serves as the substrate exit gate, because YidC is essential for bacterial viability (3, 29), and TmYidC appeared to be unable to rescue the *yidC*-depleted *E. coli* (**Fig. 2*A, B***). After a study by Jiang *et al.* (30), we made a YidC fusion protein (Ec-Tm YidC fusion) that consists of the N-terminal 325 residues of EcYidC and the C-terminal 221 residues of TmYidC (Fig. 2*A*).This Ec-Tm YidC fusion protein is able to efficiently rescue the *yidC*-depleted *E. coli*

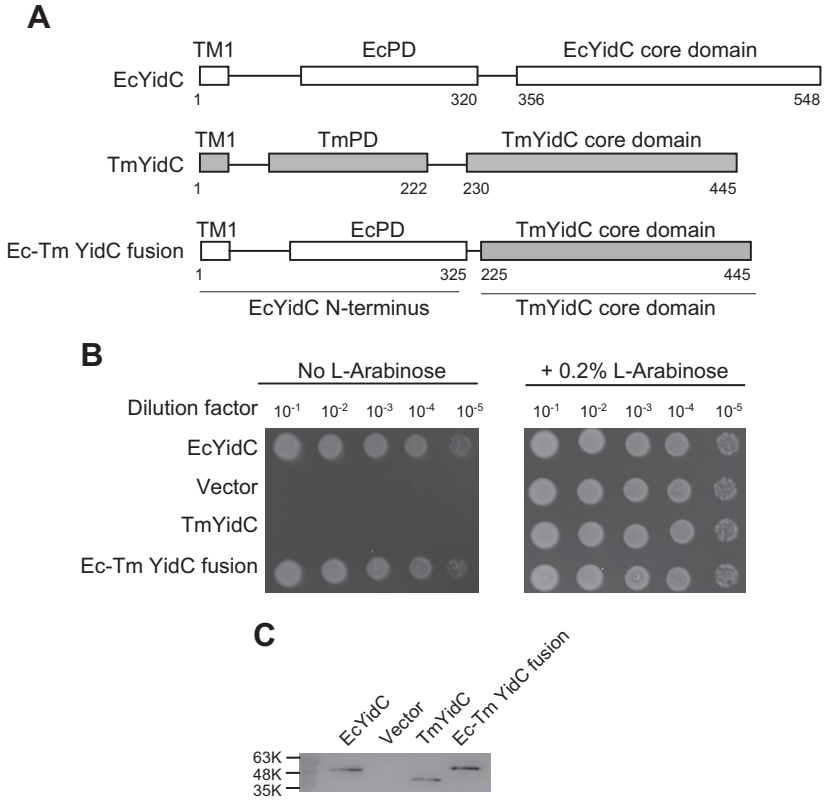


**Figure 2.** Construction of Ec-Tm YidC fusion protein for functional analysis. *A*) Schematic structures of EcYidC, TmYidC, and Ec-Tm YidC. *B*) Complementation assays showing that Ec-Tm YidC is able to rescue the *yidC*-depleted *E. coli* strain. Wild-type TmYidC is unable to rescue the *yidC*-depleted *E. coli* strain. *C*) Western blot showing the expression level of EcYidC, TmYidC, and Ec-Tm YidC in the *yidC*-depleted *E. coli* strain.

(Fig. 2*B, C*). To investigate which interface of the 2 helical bundles serves as substrate exit gate in TmYidC, we mutated residues from TM2 (L254), TM3 (F326 and R334), TM5 (F395 and L398), and TM6 (L406, L408, and T412) of Ec-Tm YidC fusion protein (**Fig. 3*A***) to crosslink the Pf3 coat protein, a Sec-independent YidC substrate, using *in vivo* photo-crosslinking experiments. In this photo-crosslinking assay, the pBPA), a photoreactive phenylalanine derivative, is incorporated into the amber codon (TAG), and the carbonyl oxygen at the benzophenone group of pBPA will react with nearby carbon-hydrogen bonds when irradiated with UV radiation. Various Ec-Tm YidC fusion mutants and its substrate Pf3 protein that was C-terminally flag-tagged were coexpressed in the *yidC*-depleted *E. coli* strain that harbors both the coexpression plasmid and the pSup-BpaRS-6TRN plasmid. The pSup-BpaRS-6TRN plasmid encodes the amber suppressor tyrosyl tRNA and tyrosyl-tRNA synthetase mutated to incorporate pBPA into an amber codon. Western blots show that residues from TM3 (F326) and TM5 (F395 and L398) that are located at the exterior surface of the TM3–TM5 interface were cross-linked to the flag-tagged Pf3 coat protein upon UV radiation (Fig. 3*B*), in a good agreement with a previous crosslinking study by Klenner and Kuhn (31). By contrast, residues from TM2 (L254) and TM6 (L408 and T412) that are located at the exterior surface of the TM2–TM6 interface did not crosslink to the Pf3 coat protein. As a positive control, residue L406 from TM6, whose side chain points to the hydrophilic groove was also crosslinked to Pf3 (16). These analyses suggest that the TM3–TM5 interface, but not the TM2–TM6 interface, serves as the sole substrate exit gate to the membrane.

## Significant rearrangement of the 2 α-helical bundles of the core domain of YidC on the periplasmic side may be necessary, to facilitate substrate integration into the membrane

In all 3-structure available YidC proteins, the conserved core domain of the YidC proteins consist of 2 loosely associated α-helical bundles that assemble to form a hydrophilic groove that is open to the cytoplasm and lipid bilayer but is kept closed at the top of the periplasmic region. To probe whether an open conformation or significant rearrangement of the 2 α-helical bundles during substrate insertion into the membrane is necessary, we engineered several disulfide bonds within the Ec–Tm YidC fusion protein with the hypothesis that intramolecular disulfide bond formation between 2 TM segments will lock their relative orientation and affect Ec-Tm YidC fusion protein mobility on nonreducing SDS-PAGE. To this end, we first selected residues L408 and T412 from TM6 and M253 from TM2. The Cα distances of M253 to that of L408 and T412 are 7.5 and 6.4 Å (**Fig. 4*A***), respectively, and this distance could allow disulfide bond formation *in vivo*. Consistent with this idea, 2 double mutants (M253C/L408C and M253C/T412C) exhibited apparently lower molecular weight on nonreducing SDS-PAGE analysis, as compared to their single-point mutants (Fig. 4*B*). By contrast, with the addition of 5 mM of the reducing reagent 2-ME to the loading dye, these double mutants returned to a position that corresponded to that of single-point mutants on SDS-PAGE (Fig. 4*C*), suggesting that these 2 double mutants formed an intramolecular disulfide bond when expressed in cells. Complementation

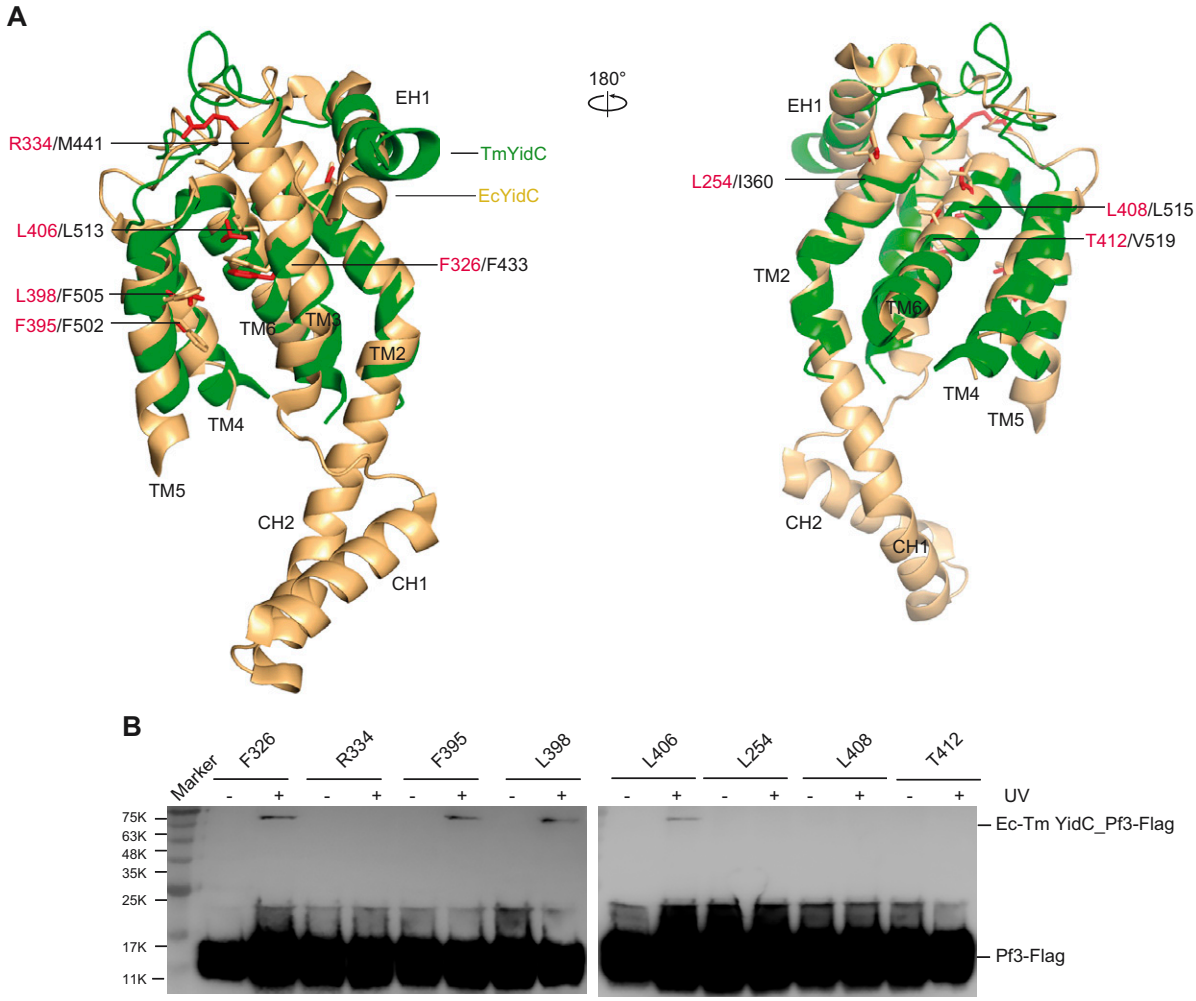


**Figure 3.** *In vivo* photo-crosslinking of Ec-Tm YidC and its substrate Pf3. *A*) Residues (shown in stick mode) at the TM2–TM6 interface and the TM3–TM5 interface were selected for a photo-crosslinking experiment. Numbers in red and in black indicate the residue (and type) in TmYidC and EcYidC, respectively. *B*) Western blot showing Ec-Tm YidC-crosslinked Pf3. Pf3 has a C-terminal Flag tag for immunoblot detection. Only residue F326 from TM3, residues F395 and L398 from TM5, and L406 from TM6 were cross-linked to Pf3 upon UV radiation. The side chain of L406 from TM6 points to the hydrophilic groove, and it was taken as a positive control in the experiment. The type and number of residues (labeled) correspond to those in the wild-type TmYidC.

assays showed that both single-point mutants (M253C, L408C, and T412C) and double mutants (M253C/L408C and M253C/T412C) of Ec-Tm YidC fusion protein effectively rescued the growth of the *yidC*-depleted *E. coli* (Fig. 4*D*), suggesting that no significant rearrangement between TM2 and -6 are necessary during substrate integration into the membrane in this region. This observation also corroborated with our finding that the TM2–TM6 interface is not the substrate exit gate as disulfide bond formation should not allow substrate laterally exit to the membrane through the TM2–TM6 interface. Next, using a similar strategy, we tested whether rearrangement of the 2 loosely packed α-helical bundles is required for substrate integration into membrane. To test this, we mutated residue L402, which is located on the E3 loop in the α-helical bundle II, and residue W330 from TM3 in the α-helical bundle I to cysteine (Fig. 4*A*). The Cα–Cα distance between these 2 residues is 7.8 Å. SDS-PAGE analysis indicated that this double mutant (L402C/W330C) of Ec-Tm YidC fusion protein also contains intramolecular disulfide bond, given that the double-mutant protein has a rapid mobility on SDS-PAGE under a nonreducing condition (Fig. 4*B*, *C*). In contrast to single-point mutants (L402C and W330C), complementation assays showed that the double mutant (L402C/W330C) was unable to rescue the growth of the *yidC*-depleted *E. coli* (Fig. 4*D*), suggesting that significant rearrangement of the 2 α-helical bundles may be necessary during substrate insertion into the membrane.

## DISCUSSION

YidC proteins have been reported to participate in a range of cellular reactions, including ribosome and signal recognition particle binding, SecYEG translocon interactions, and insertion, folding, and oligomerization of its substrates. Despite great progress made recently in understanding the structure and function of YidC proteins, the exact molecular mechanisms of YidC-mediated membrane protein biogenesis are not fully understood. In

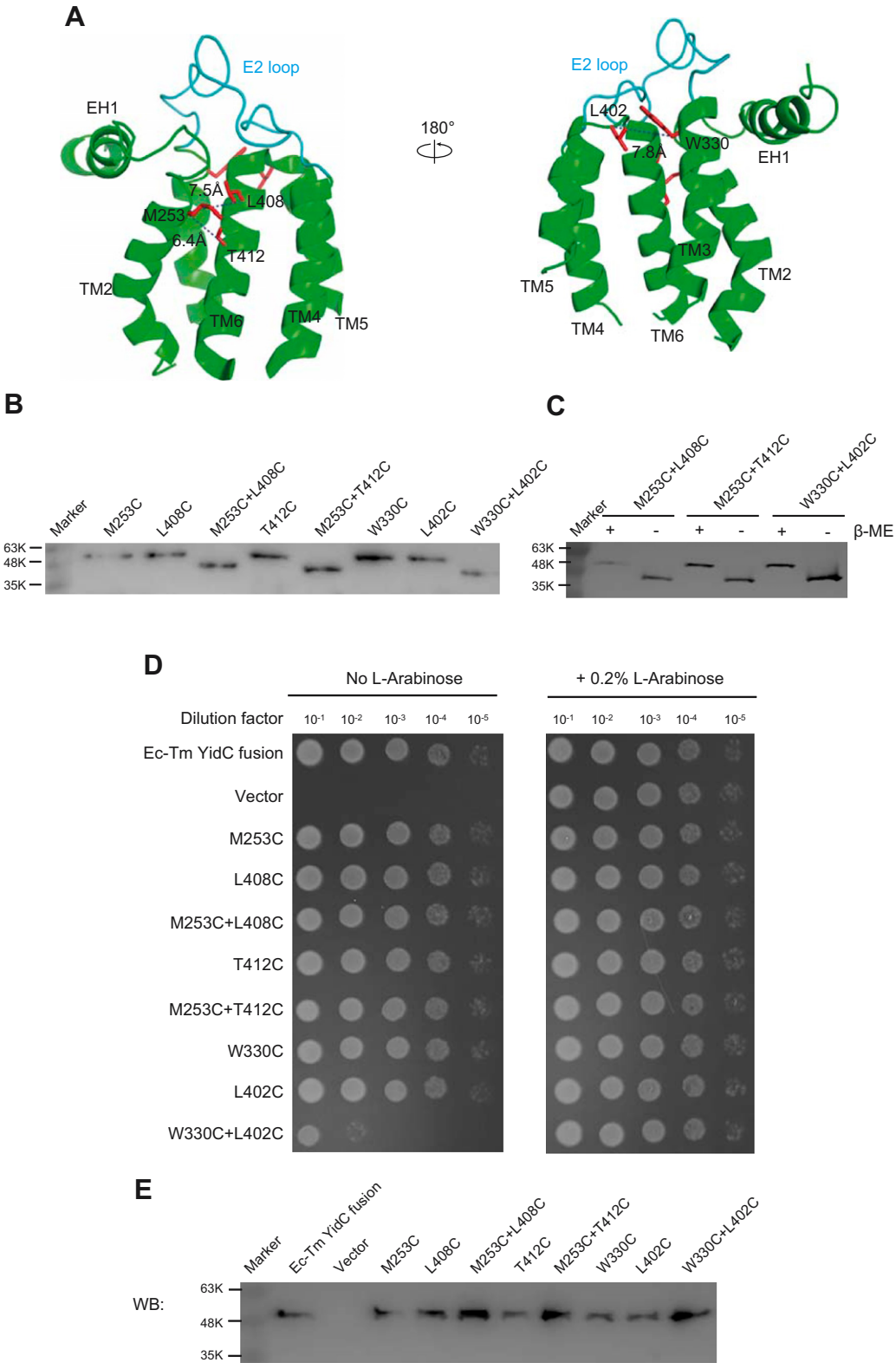


**Figure 4.** Intramolecular disulfide bond formation and its effects on the growth of the *yidC*-depleted *E. coli*. *A*) Close-up view of selected residues for intramolecular disulfide bond formation. *B*) Disulfide bond formation affects Ec-Tm YidC mobility on nonreducing 12% SDS-PAGE. *C*) Addition of 2-ME disrupted intramolecular disulfide bond in Ec-Tm YidC and affected its mobility on 12% SDS-PAGE. *D*) Growth phenotypes of the *yidC*-depleted *E. coli* when complemented with mutant Ec-Tm YidC. *E*) Western blot showing the relative protein expression levels of the wild-type Ec-Tm YidC and various Ec-Tm YidC mutants. The type and number of residues (labeled) correspond to those in the wild-type TmYidC.

this study, we reported the crystal structures of the TmPD, as well as the full-length TmYidC, that was crystallized in a detergent-solubilized state. The first crystal structure of YidC proteins in a detergent-solubilized state is the archaeal YidC-like protein DUF106 from *M. jannaschii* (Mj0480). Distinct from the DUF106 protein that forms tetramers in a detergent-solubilized state, TmYidC forms monomers and its conserved C-terminal core domain closely resembles that of BhYidC and EcYidC but not the DUF106 protein. Our study presents the first crystal structure of YidC proteins that form monomers in a detergent-solubilized state and further supports the notion that YidC proteins function as monomers *in vivo*. The findings that TmYidC adopts monomers in a detergent-solubilized state, and the structural conservation in the C-terminal core domain between TmYidC and EcYidC and BhYidC indicates that detergents may not affect the oligomerization state and conformational state of the YidC proteins.

Using *in vivo* photo-crosslinking experiments, we further showed that only residues from the exterior surface of the TM3–TM5 interface but not from the TM2–TM6 interface, are able to crosslink to YidC substrate Pf3, demonstrating that the TM3–TM5 interface is the potential substrate exit gate during substrate integration into membrane. Supporting this hypothesis, intramolecular disulfide bond formation between TM2 and -6 in the α-helical bundle II of EcYidC did not affect the growth of the *yidC*-depleted *E. coli* strain. By contrast, an engineered disulfide bond that potentially fixes the relative orientation of the 2 α-helical bundles on the periplasmic side is deleterious to YidC function, suggesting that significant rearrangement of the 2 α-helical bundles on the periplasmic region occurs, whereas no remarkable conformational changes within the α-helical bundle II are necessary during substrate insertion into the lipid bilayer. This observation is also in part consistent with a previous study showing that large conformational changes of the TM segments of EcYidC took place upon binding of substrate to YidC *in vitro* (19).

Our study provides more insights in understanding YidC-mediated membrane protein biogenesis, yet a deep mechanical understanding of YidC function awaits a further structural snapshot of the YidC protein in complex with its native substrate. Fj

## ACKNOWLEDGMENTS

The authors thank all Y.H. laboratory staff members for valuable discussions and critically reading the manuscript. The diffraction data were collected at the Shanghai Synchrotron Radiation Facility (SSRF). This work was supported by Grants 2016YFA0500404 and 2013CB910603 from the Ministry of Science and Technology (to Y.H.); Grants 31625009 and 31470743 from the National Natural Science Foundation of China (to Y.H.), and Grant XDB080203 from the Strategic Priority Research Program of the Chinese Academy of Sciences (to Y.H.). The coordinates and diffraction data of TmPD and TmYidC crystal structures have been deposited in the Research Collaboratory for Structural Bioinformatics Protein Data Bank (RCSB PDB; *http://rcsb.org*; 5Y82 and 5Y83). The authors declare no conflicts of interests.

## AUTHOR CONTRIBUTIONS

Y. Huang supervised the project; Y. Xin, Y. Zhao, J. Zheng, and H. Zhou performed the experiments; Y. Xin and Y. Zhao collected diffraction data; Y. Xin and Y. Zhao built the model and refined the structure; Y. Xin, J. Zheng, X. C. Zhang, C. Tian, and Y. Huang contributed to manuscript preparation; Y. Xin, X. C. Zhang, C. Tian, and Y. Huang wrote the manuscript; and all authors contributed to data analysis.

## REFERENCES

1. Veenendaal, A. K., van der Does, C., and Driessen, A. J. (2004) The protein-conducting channel SecYEG. *Biochim. Biophys. Acta* **1694**, 81–95
2. Schuldiner, M., Metz, J., Schmid, V., Denic, V., Rakwalska, M., Schmitt, H. D., Schwappach, B., and Weissman, J. S. (2008) The GET complex mediates insertion of tail-anchored proteins into the ER membrane. *Cell* **134**, 634–645
3. Saller, M. J., Wu, Z. C., de Keyzer, J., and Driessen, A. J. (2012) The YidC/Oxa1/Alb3 protein family: common principles and distinct features. *Biol. Chem.* **393**, 1279–1290
4. Funes, S., Kauff, F., van der Sluis, E. O., Ott, M., and Herrmann, J. M. (2011) Evolution of YidC/Oxa1/Alb3 insertases: three independent gene duplications followed by functional specialization in bacteria, mitochondria and chloroplasts. *Biol. Chem.* **392**, 13–19
5. Wang, P., and Dalbey, R. E. (2011) Inserting membrane proteins: the YidC/Oxa1/Alb3 machinery in bacteria, mitochondria, and chloroplasts. *Biochim. Biophys. Acta* **1808**, 866–875
6. Dalbey, R. E., Kuhn, A., Zhu, L., and Kiefer, D. (2014) The membrane insertase YidC. *Biochim. Biophys. Acta* **1843**, 1489–1496
7. Schulze, R. J., Komar, J., Botte, M., Allen, W. J., Whitehouse, S., Gold, V. A., Lycklama A Nijeholt, J. A., Huard, K., Berger, I., Schaffitzel, C., and Collinson, I. (2014) Membrane protein insertion and proton-motive-force-dependent secretion through the bacterial holotranslocon SecYEG-SecDF-YajC-YidC. *Proc. Natl. Acad. Sci. USA* **111**, 4844–4849
8. Jiang, F., Chen, M., Yi, L., de Gier, J. W., Kuhn, A., and Dalbey, R. E. (2003) Defining the regions of Escherichia coli YidC that contribute to activity. *J. Biol. Chem.* **278**, 48965–48972
9. Oliver, D. C., and Paetzel, M. (2008) Crystal structure of the major periplasmic domain of the bacterial membrane protein assembly facilitator YidC. *J. Biol. Chem.* **283**, 5208–5216
10. Ravaud, S., Stjepanovic, G., Wild, K., and Sinning, I. (2008) The crystal structure of the periplasmic domain of the Escherichia coli membrane protein insertase YidC contains a substrate binding cleft. *J. Biol. Chem.* **283**, 9350–9358
11. Seitl, I., Wickles, S., Beckmann, R., Kuhn, A., and Kiefer, D. (2014) The C-terminal regions of YidC from Rhodopirellula baltica and Oceanicaulis alexandrii bind to ribosomes and partially substitute for SRP receptor function in Escherichia coli. *Mol. Microbiol.* **91**, 408–421
12. Kohler, R., Boehringer, D., Greber, B., Bingel-Erlenmeyer, R., Collinson, I., Schaffitzel, C., and Ban, N. (2009) YidC and Oxa1 form dimeric insertion pores on the translating ribosome. *Mol. Cell* **34**, 344–353
13. Herrmann, J. M. (2013) The bacterial membrane insertase YidC is a functional monomer and binds ribosomes in a nascent chain-dependent manner. *J. Mol. Biol.* **425**, 4071–4073
14. Kedrov, A., Sustarsic, M., de Keyzer, J., Caumanns, J. J., Wu, Z. C., and Driessen, A. J. (2013) Elucidating the native architecture of the YidC: ribosome complex. *J. Mol. Biol.* **425**, 4112–4124
15. Kumazaki, K., Chiba, S., Takemoto, M., Furukawa, A., Nishiyama, K., Sugano, Y., Mori, T., Dohmae, N., Hirata, K., Nakada-Nakura, Y., Maturana, A. D., Tanaka, Y., Mori, H., Sugita, Y., Arisaka, F., Ito, K., Ishitani, R., Tsukazaki, T., and Nureki, O. (2014) Structural basis of Sec-independent membrane protein insertion by YidC. *Nature* **509**, 516–520

16. Kumazaki, K., Kishimoto, T., Furukawa, A., Mori, H., Tanaka, Y., Dohmae, N., Ishitani, R., Tsukazaki, T., and Nureki, O. (2014) Crystal structure of Escherichia coli YidC, a membrane protein chaperone and insertase. *Sci. Rep.* **4**, 7299
17. Borowska, M. T., Dominik, P. K., Anghel, S. A., Kossiakoff, A. A., and Keenan, R. J. (2015) A YidC-like protein in the archaeal plasma membrane. *Structure* **23**, 1715–1724
18. Kuhn, A., and Kiefer, D. (2017) Membrane protein insertase YidC in bacteria and archaea. *Mol. Microbiol.* **103**, 590–594
19. Winterfeld, S., Imhof, N., Roos, T., Bär, G., Kuhn, A., and Gerken, U. (2009) Substrate-induced conformational change of the Escherichia coli membrane insertase YidC. *Biochemistry* **48**, 6684–6691
20. Otwinowski, Z., and Minor, W. (1997) Processing of X-ray diffraction data collected in oscillation mode. *Methods Enzymol.* **276**, 307–326
21. Sheldrick, G. M. (2008) A short history of SHELX. *Acta Crystallogr. A* **64**, 112–122
22. Adams, P. D., Grosse-Kunstleve, R. W., Hung, L. W., Ioerger, T. R., McCoy, A. J., Moriarty, N. W., Read, R. J., Sacchettini, J. C., Sauter, N. K., and Terwilliger, T. C. (2002) PHENIX: building new software for automated crystallographic structure determination. *Acta Crystallogr. D Biol. Crystallogr.* **58**, 1948–1954
23. Emsley, P., and Cowtan, K. (2004) Coot: model-building tools for molecular graphics. *Acta Crystallogr. D Biol. Crystallogr.* **60**, 2126–2132
24. DeLano, W. L. PyMOL 2.0 Available at https://pymol.org/2/. Accessed December 4, 2017
25. Datsenko, K. A., and Wanner, B. L. (2000) One-step inactivation of chromosomal genes in Escherichia coli K-12 using PCR products. *Proc. Natl. Acad. Sci. USA* **97**, 6640–6645
26. Sachelaru, I., Petriman, N. A., Kudva, R., Kuhn, P., Welte, T., Knapp, B., Drepper, F., Warscheid, B., and Koch, H. G. (2013) YidC occupies the lateral gate of the SecYEG translocon and is sequentially displaced by a nascent membrane protein. *J. Biol. Chem.* **288**, 16295–16307
27. Xie, K., Kiefer, D., Nagler, G., Dalbey, R. E., and Kuhn, A. (2006) Different regions of the nonconserved large periplasmic domain of Escherichia coli YidC are involved in the SecF interaction and membrane insertase activity. *Biochemistry* **45**, 13401–13408
28. Shimokawa-Chiba, N., Kumazaki, K., Tsukazaki, T., Nureki, O., Ito, K., and Chiba, S. (2015) Hydrophilic microenvironment required for the channel-independent insertase function of YidC protein. *Proc. Natl. Acad. Sci. USA* **112**, 5063–5068
29. Samuelson, J. C., Chen, M., Jiang, F., Möller, I., Wiedmann, M., Kuhn, A., Phillips, G. J., and Dalbey, R. E. (2000) YidC mediates membrane protein insertion in bacteria. *Nature* **406**, 637–641
30. Jiang, F., Yi, L., Moore, M., Chen, M., Rohl, T., Van Wijk, K. J., De Gier, J. W., Henry, R., and Dalbey, R. E. (2002) Chloroplast YidC homolog Albino3 can functionally complement the bacterial YidC depletion strain and promote membrane insertion of both bacterial and chloroplast thylakoid proteins. *J. Biol. Chem.* **277**, 19281–19288
31. Klenner, C., and Kuhn, A. (2012) Dynamic disulfide scanning of the membrane-inserting Pf3 coat protein reveals multiple YidC substrate contacts. *J. Biol. Chem.* **287**, 3769–3776

*Received for publication August 23, 2017.*
*Accepted for publication December 4, 2017.*